Journal of Materials, Processing and Design (2022)
Clausius Scientific Press, Canada
DOI: 10.23977/jmpd.2022.060209
ISSN 2516-0923 Vol. 6 Num. 2

Discussion about the "Modified-B.E.P." Model of Near Surface Mounted CFRP Strengthening Concrete

Xiaodong Zhang

School of Environmental Arts and Architectural Engineering, Heilongjiang University of Technology, No.99 South Heping Street, Jixi City, Heilongjiang Province, China

Keywords: Near Surface Mounted CFRP, Stress-Slip Model, Strengthening Concrete

Abstract: During the last decade, conventional materials such as steel have been replaced by fibre-reinforced polymer (FRP) material for the strengthening of the concrete structures. Although externally bonded FRP reinforcement performed extremely well in practice, premature debonding failure was observed and identified by many researchers. To solve the problem, the method of near-surface mounted FRP rods was adopted. This technique becomes particularly attractive for flexural strengthening in the negative moment regions of slabs and decks, where external reinforcement would be subjected to mechanical and environmental damage and would require protective cover, which could interfere with the presence of floor finishes.

1. Introduction

In the paper of Francesco Focacci, Antonio Nanni and Charles E. Bakis (2000) named "Local Bond-Slip Relationship for FRP Reinforcement in Concrete", a method for the determination of the parameters of a local $\tau=\tau(s)$ relationship from results of pull-out tests that make into account the distribution of slip and bond shear stress along the embedded portion of the bar was proposed [1]. This method was applied to some pull-out test results, corresponding to different embedded lengths, and local $\tau=\tau(s)$ relationships were found. Based on this method, different researchers have different conclusions in terms of the relationship between shear stress and loaded end slip, such as the "Tri-Linear" model, the "BEP" model, the "Modified-B.E.P." model, the "CMR" model, the "Naaman" model and the "Malvar" model. Among these models, the "Modified-B.E.P." model is used wider. In the paper, we are going to discuss the application of the "Modified-B.E.P." model [2].

2. The "Modified-B.E.P." model

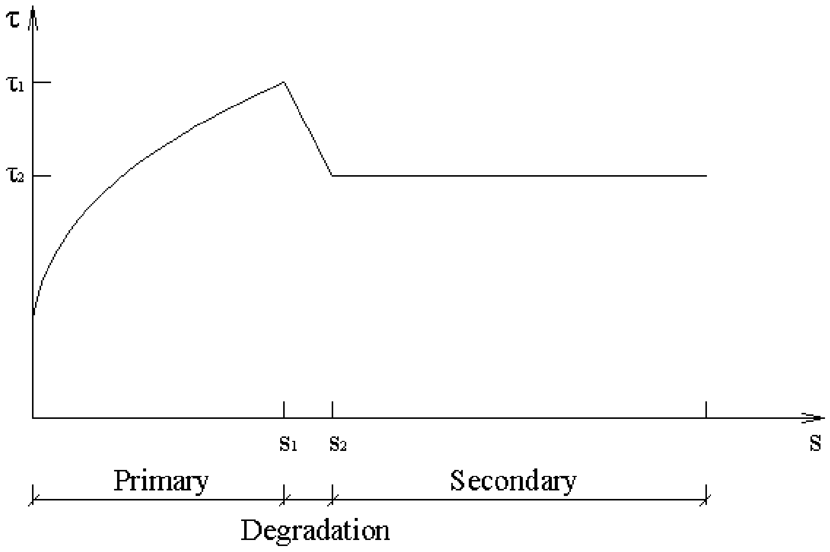

Figure 1: The Modified-B.E.P. model

There are three parts in the Modified-B.E.P. model (Figure 1) [3]:

• A non-linear ascending branch, of the form ($s<s_1$) [Primary zone]:

$$\frac{\tau}{\tau_1} = (\frac{s}{s_1})^{\Omega} \quad \text{or} \quad \tau = \rho_1 s^{\Omega} \tag{1}$$

Ω describes the shape of the ascending branch, τ_1 is the peak shear stress and s_1 is the corresponding slip and $\rho_1 = \tau_1 / s^{\Omega}$.

• A linear descending branch, describing degradation of the concrete- reinforcement bond ($s_1<s<s_2$) [Degradation zone]:

$$\tau = \tau_1 + \frac{\tau_2 - \tau_1}{s_2 - s_1}(s - s_1) \quad \text{or} \quad \tau = \rho_2 - \rho_3 s \tag{2}$$

Where, $\rho_2 = \frac{s_2\tau_1 - s_1\tau_2}{s_1 - s_2}$ and $\rho_3 = \frac{\tau_1 - \tau_2}{s_2 - s_1}$

- A constant shear stress, representing residual friction ($s_2<s$) [Secondary zone]:

$$\tau = \tau_2 \tag{3}$$

The values of σ_1, σ_2, σ_3 and Ω are parameters to be found.

3. Application of the Modified-B.E.P. model

3.1 Governing equations for the Modified-B.E.P. model

3.1.1 General governing equation for reinforcement-concrete bond

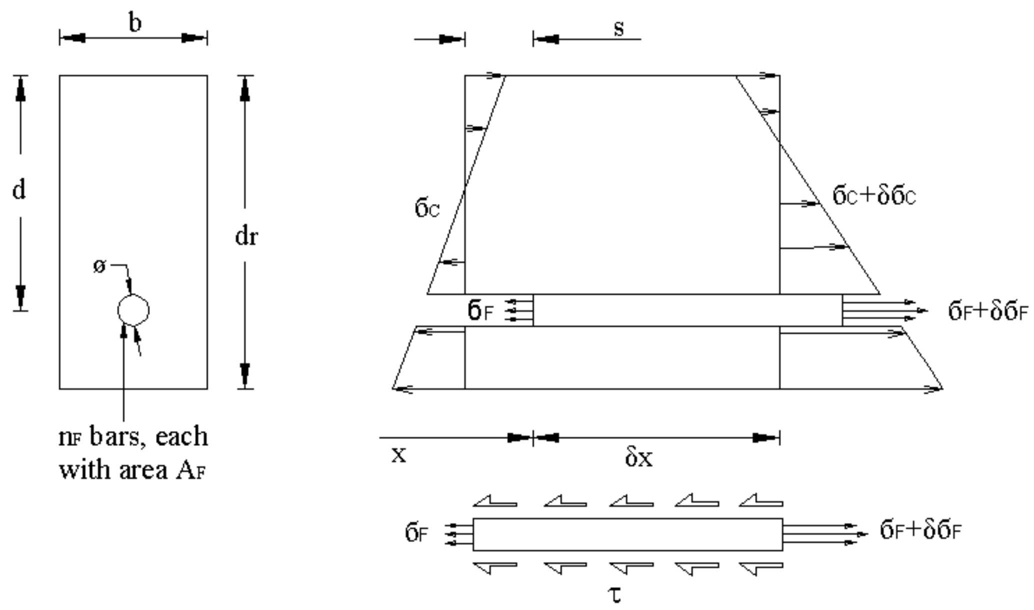

Figure 2: Short embedded length specimen, for deriving governing equation

The slip (s) of the reinforcement is the relative displacement between the concrete (U_C) and the reinforcement (U_F):

$$s = U_F - U_C \tag{4}$$

The differentiation of U_C and U_F with respect to the position gives the changes of strain in reinforcement and concrete after being bonded [3]. Writing the total strain in the concrete and reinforcement as ε_C and ε_F, then:

$$\frac{ds}{dx} = \frac{dU_F}{dx} - \frac{dU_C}{dx} \text{ (no pre-load in the reinforcement)} \tag{5}$$

For, $$\frac{dU_C}{dx} = \varepsilon_C \text{ and } \frac{dU_F}{dx} = \varepsilon_F \text{ (no pre-load in the reinforcement)}$$

So, $$\frac{ds}{dx} = \varepsilon_F - \varepsilon_C \text{ (no pre-load in the reinforcement)} \tag{6}$$

In terms of stress:

$$\frac{ds}{dx} = \frac{\sigma_F}{E_F} - \frac{\sigma_C}{E_C} \tag{7}$$

Equation (7) can be differentiated again [4]:

$$\frac{d^2 s}{dx^2} = \frac{1}{E_F}\frac{d\sigma_F}{dx} - \frac{1}{E_C}\frac{d\sigma_C}{dx} \tag{8}$$

Where: E_F – Young's modulus of the reinforcement
E_C – Young's modulus of the concrete
σ_F – stress of the reinforcement
σ_C – stress of the concrete

In Figure 2, the changes in the concrete stress ($\delta\sigma_C$) to changes in the reinforcement ($\delta\sigma_F$) are related by the horizontal equilibrium of the specimen (or by equation (8)):

- For the concrete, assuming that it forms a plane section:

$$\delta\sigma_C = -\frac{4n_F A_F}{bd_T{}^3}\{d_T{}^2 + 3d(d - d_T)\}\delta\sigma_F \tag{9}$$

Substitute equation (9) back into equation (8):

$$\frac{d^2 s}{dx^2} = [\frac{1}{E_F} + \frac{4n_F A_F}{bd_T{}^3 E_C}\{d_T{}^2 + 3d(d - d_T)\}]\frac{d\sigma_F}{dx} \tag{10}$$

- For the reinforcement (Figure 2), the bond stress (τ):

$$\tau = \frac{\phi}{4}\frac{d\sigma_F}{dx} \tag{11}$$

Substitute equation (11) back into equation (10):

$$\frac{d^2 s}{dx^2} = K\tau \tag{12}$$

Where:

$$K = \frac{4}{\phi E_F}[1 + \frac{4n_F A_F E_F}{bd_T{}^3 E_C}\{d_T{}^2 + 3d(d - d_T)\}] \tag{13}$$

K describes the section properties of the specimen. If a single reinforcement ($n_F = 1$) is placed at the centre of the specimen ($d = d_T/2$), K simplifies to:

$$K_{CE} = \frac{4}{\phi E_F}[1 + \frac{A_F E_F}{bd_T E_C}] \tag{14}$$

The plane-sections assumption is unlikely to be valid, so for eccentrically placed reinforcement K is likely to be somewhere between these two values. Ciampi et al.[5] assumed that the concrete deformation is negligible, giving $K_{CE}=4/(\phi E_F)$.

Equation (12) is the general governing equation for reinforcement-concrete bond. It expresses equilibrium and compatibility requirements across the interface between the concrete and the reinforcement, but does not assume a particular τ-s model.

3.1.2 The governing equation for the Modified-B.E.P. model

Substitute equation (1), (2) & (3) back into equation (12) separately give the governing equation for the Modified-B.E.P. model:

- Primary zone ($s<s_1$): $$\frac{d^2s}{dx^2} = K\tau_1(\frac{s}{s_1})^{\Omega} = K\rho_1 s^{\Omega} \quad (15)$$
- Degradation zone ($s_1<s<s_2$): $$\frac{d^2s}{dx^2} = K\{\tau_1 + \frac{\tau_2 - \tau_1}{s_2 - s_1}(s - s_1)\} = K(\rho_2 - \rho_3 s) \quad (16)$$
- Secondary zone ($s_2<s$): $$\frac{d^2s}{dx^2} = K\tau_2 \quad (17)$$

The values of σ_1, σ_2, σ_3 and Ω are parameters to be found.

3.2 Boundary conditions for long embedded length directly pull-out test

Typically there are two types of loading arrangements: one is the directly pull-out test in which only one end of the embedded length is loaded and the other is the beam pull-out test in which the embedded length is usually bonded by two cracks, and both ends of the embedded are loaded. Since the directly pull-out test is adopted in this thesis project, only the first loading arrangement (Figure 3) is considered in this section.

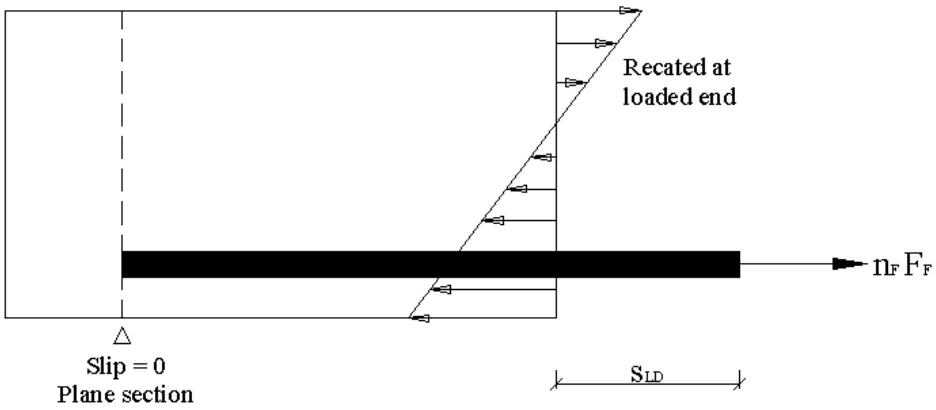

Figure 3: Stress reacted at the loaded end

For there is no pre-load applied to the reinforcement while it was being bonded, the effect of the pre-stress in the reinforcement will not be considered here.

The target of the boundary conditions is to allow the governing equations to be solved for pull-out test. Generally it is applied to four special positions [6]:

- The loaded end – one end of the embedded length to which the load was applied.
- The free end – the other end of the embedded length where no load applied.
- The end of the disturbed length – the end of the reinforcement along which slip occurs.
- Transitions between different parts of the constitutive model – the constitutive model (Modified-B.E.P. model in this thesis) is a continuous curve that is composed of three different parts, and character of the connecting point of two different parts is selected as the boundary conditions.

3.2.1 Boundary conditions at the loaded end

$$s = s_{LD} \tag{18}$$

For the reinforcement, if the applied load is F and the cross-sectional area is A_F, the stress of it is:

$$\sigma_F = \frac{F}{A_F} \tag{19}$$

In the directly pull-out test, since all the load is applied to one end of the embedded length, the reacted load is given by the concrete at the loaded end. The concrete stress at the level of the reinforcement could be derived from equilibrium as [7]:

$$\sigma_C = -\frac{4n_F F}{bd_T^{\ 3}}\{d_T^{\ 2} + 3d(d - d_T)\} \tag{20}$$

For a single reinforcement ($n_F = 1$) which is placed at the centre of the specimen ($d_T/2 = d$), σ_C simplifies to:

$$\sigma_C = -\frac{F}{bd_T} \tag{21}$$

Substitute equation (19) and (21) back into equation (7) gives:

$$\frac{ds}{dx} = \frac{F}{A_F E_F} + \frac{F}{A_C E_C} \tag{22}$$

Where, $$A_C = bd_T \tag{23}$$

(**Note**: Equation (22) above is derived under the condition that a *single* reinforcement is placed at the *centre* of the specimen *without* any pre-load applied on it, and this kind of condition is suitable for the direct pull-out tests of this thesis project).

If the reinforcement is pull-out through the concrete without any significant crack on the surface, the $\frac{ds}{dx}$ relationship at the loaded end must satisfy equation (22), but if it is pull-out from the surface of a crack:

$$\sigma_C = 0 \tag{24}$$

(24) and (7) give $$\frac{ds}{dx} = \frac{F}{A_F E_F} \quad \text{(no pre-load)} \tag{25}$$

3.2.2 Boundary conditions at the free end

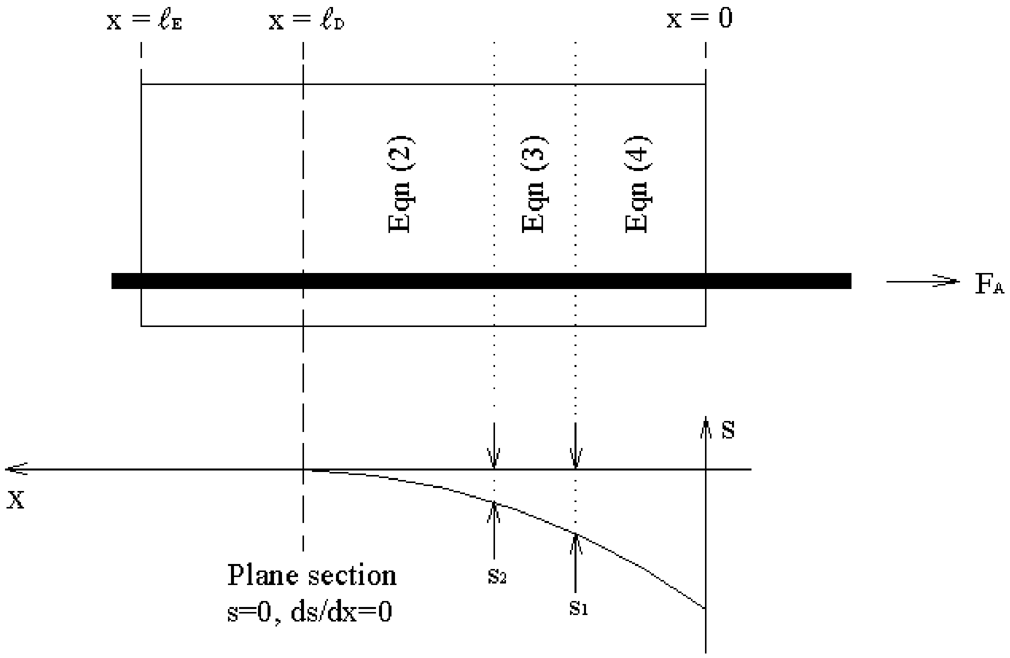

Figure 4: $\ell_D < \ell_E$, no slip at the free end

As the load applied on the reinforcement increases, the length of the reinforcement along which slip occurs from the loaded end (disturbed length ℓ_E) increases until it equals to the embedded length (ℓ_D) and slip occurs at the free end. So there are two situations for the free end [8]:

a) If $\ell_D < \ell_E$ (Figure 4)

Since the free end has not been disturbed yet:

$$s = 0 \tag{26}$$

Concrete and reinforcement forms plane section, so:

$$\varepsilon_C = \varepsilon_F \quad \text{(no pre-load)} \tag{27}$$

(27) and (6) give
$$\frac{ds}{dx} = 0 \tag{28}$$

b) If $\ell_D = \ell_E$

In this situation, the boundary conditions applied to the loaded end can also be applied here. So, if no significant crack occurs, the $\frac{ds}{dx}$ relationship also satisfies equation (22), and because the applied force is (F) is zero, the value of $\frac{ds}{dx}$ is equal to zero.

3.2.3 Boundary conditions at the end of the disturbed length

The disturbed length increases with the applied load until the end of the disturbed length reaches to the free end. At the end of the disturbed length, the concrete and reinforcement form a plane section (Figure 4) before the end of the disturbed length reaches to the free end, so:

$$\varepsilon_C = \varepsilon_F \qquad (27)\text{bis}$$

(27) and (7) give
$$\frac{ds}{dx} = 0 \qquad (28)\text{bis}$$

3.2.4 Boundary conditions at transitions between different parts of the constitutive model

Since the constitutive model (Modified-B.E.P. model in this thesis) is a continuous curve with three parts that are governed by three different equations separately, the character of the connecting point of different parts could be a proper boundary condition.

The constitutive model is continuous, so the two parameters in the model must be continuous:

- The stress expressed by ds/dx (equation 11) must be continuous.
- The slip(s) must be continuous.

3.3 Solutions of the governing equations for long-embedded-length specimen

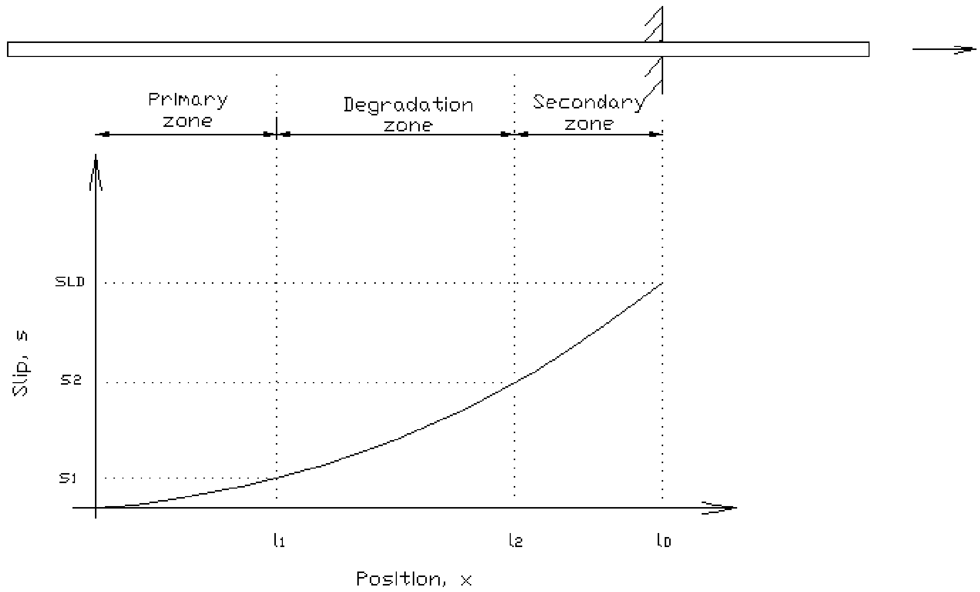

Figure 5: Slip distribution according to the Modified-B.E.P. model

There are three zones in the Modified-B.E.P. model which are governed by three different equations (1), (2) and (3) separately. As the tensile load is increased, the disturbed length increases and different zones present.

Different zones will present at different ranges of loaded end slip (s_{LD}) (Figure 5) [9]

- $s_{LD}<s_1$, Only primary zone present
- $s_1<s_{LD}<s_2$, Primary and degradation zones present
- $s_2<s_{LD}$, Primary, secondary and degradation zones present

So, solutions of the governing for the three ranges of loaded end slips are required separately.

3.3.1 Only primary zone present

If the range of the loaded end slip is $s_{LD}<s_1$, only the primary zone presents. The governing equation of the primary zone is:

$$\frac{d^2 s}{dx^2} = K\rho_1 s^{\Omega} \tag{15)bis}$$

Where, $$K = K_{CE} = \frac{4}{\phi E_F}[1+\frac{A_F E_F}{A_C E_C}] \text{ (for the situation of this thesis)} \quad (14)\text{bis}$$

(14), (15) give $$\frac{d^2 s}{dx^2} = K_{CE}\rho_1 s^{\Omega} \quad (29)$$

The boundary condition at the free end ($x = 0$) of the CFRP rod, $s = 0$ and $dx/ds = 0$ can be used to solve the governing equation:

$$s = [\frac{K_{CE}\rho_1(1-\Omega)^2}{2(1+\Omega)}]^{\frac{1}{1-\Omega}} x^{\frac{2}{1-\Omega}} \quad (30)$$

At the loaded end ($x = \ell_D$) of the CFRP rod, the disturbed length can be derived from the boundary condition (18), so:

(30) gives $$\ell_D = \sqrt{\frac{2(1+\Omega)}{K_{CE}\rho_1(1-\Omega)^2}} s_{LD}^{\frac{1-\Omega}{2}} \quad (31)$$

The tensile load applied (F) causing the slip can be found by the loaded end boundary condition (22):

(30), (31), (22) give $$(\frac{ds}{dx})_{LD} = \sqrt{\frac{2\rho_1 K_{CE}}{1+\Omega}} s_{LD}^{\frac{1+\Omega}{2}} = \frac{F}{A_F E_F} + \frac{F}{A_C E_C} \quad (32)$$

(32) gives $$F = \frac{A_F E_F A_C E_C}{A_C E_C + A_F E_F}\sqrt{\frac{2\rho_1 K_{CE}}{1+\Omega}} s^{\frac{1+\Omega}{2}} \quad (33)$$

Equation (33) above is suitable for the particular situation of this thesis: for each of the tests, a single CFRP rod ($n_F = 1$) is placed at the centre of the specimens ($d = d_T/2$) and no pre-load ($P = 0$) is applied on it.

3.3.2 Primary zone and degradation zones present

When the slip of loaded end exceeds s_1, the degradation zone comes up but the length and shape of the primary zone (ℓ_1) stays constant [10]:

(31) gives $$\ell_1 = \sqrt{\frac{2(1+\Omega)}{K_{CE}\rho_1(1-\Omega)^2}} s_{LD}^{\frac{1-\Omega}{2}} \quad (34)$$

At the boundary between the primary and degradation zones:

(32) gives $$(\frac{ds}{dx})_{L1} = \sqrt{\frac{2\rho_1 K_{CE}}{1+\Omega}} s_{LD}^{\frac{1+\Omega}{2}} \quad (35)$$

The degradation zone is governed by equation (16) which is looked like:

$$\frac{d^2s}{dx^2} = K(\rho_2 - \rho_3 s) \tag{16)bis}$$

Where, $$K = K_{CE} = \frac{4}{\phi E_F}[1 + \frac{A_F E_F}{A_C E_C}]$$ (for the situation of this thesis) (14)bis

(14), (16) give $$\frac{d^2s}{dx^2} = K_{CE}(\rho_2 - \rho_3 s) \tag{36}$$

The equation (36) is solved to get:

$$s = B_1 \sin(\sqrt{K_{CE}\rho_3}\,x) + B_2 \cos(\sqrt{K_{CE}\rho_3}\,x) + \frac{\rho_2}{\rho_3} \tag{37}$$

B_1 and B_2 are constants which are required for continuity of s and ds/dx at the boundary with primary zone ($x = \ell_1$):

(35) gives (38)

$$B_1 = \sqrt{\frac{2\rho_1}{\rho_3(1+\Omega)}}\,s_1^{\frac{1+\Omega}{2}} \cos(\sqrt{K_{CE}\rho_3}\,\ell_1) - \frac{\tau_1}{\rho_3}\sin(\sqrt{K_{CE}\rho_3}\,\ell_1)$$

$$B_2 = \sqrt{\frac{2\rho_1}{\rho_3(1+\Omega)}}\,s_1^{\frac{1+\Omega}{2}} \frac{(\cos^2(\sqrt{K_{CE}\rho_3}\,\ell_1) - 1)}{\sin(\sqrt{K_{CE}\rho_3}\,\ell_1)} - \frac{\tau_1}{\rho_3}\cos(\sqrt{K_{CE}\rho_3}\,\ell_1)$$

Use the loaded end boundary condition equations (18), (22):

(18) gives $$s_{LD} = B_1 \sin(\ell_D\sqrt{K_{CE}\rho_3}) + B_2 \cos(\ell_D\sqrt{K_{CE}\rho_3}) + \frac{\rho_2}{\rho_3} \tag{39}$$

(22) gives:

$$(\frac{ds}{dx})_{LD} = \sqrt{K_{CE}\rho_3}[B_1 \cos(\ell_D\sqrt{K_{CE}\rho_3}) - B_2 \sin(\ell_D\sqrt{K_{CE}\rho_3})] = \frac{F}{A_F E_F} + \frac{F}{A_C E_C} \tag{40}$$

Depending on whether s_{LD} or F is known, (39) or (40) is solved to give the disturbed length (ℓ_D), and the unknown variables is found from the unused equation .

It is useful to note that for:

$$a\sin\theta + b\cos\theta = c, \qquad \theta = 2\tan^{-1}(\frac{a \pm \sqrt{a^2 + b^2 - c^2}}{b+c}) + 2\pi.j \tag{41}$$

The disturbed length can be found from the loaded end slip:

(40) gives

$$\ell_D = \frac{2}{\sqrt{K_{CE}\rho_3}}\tan^{-1}[\frac{B_1 - \sqrt{B_1^2 + B_2^2 - (s_{LD} - \rho_2/\rho_3)^2}}{B_2 + s_{LD} - \rho_2/\rho_3}] + \frac{2\pi.j}{\sqrt{K_{CE}\rho_3}} \tag{42}$$

For ds/dx is positive, the negative root is used. j is chosen to give the first solution with $\ell_D > \ell_1$. F is found from equation (40).

The disturbed length can also be calculated from the applied load:

(39) gives

$$\ell_D = \frac{2}{\sqrt{K_{CE}\rho_3}} \tan^{-1}\left[\frac{-B_2 - \sqrt{B_1^{\,2} + B_2^{\,2} - \frac{1}{K_{CE}\rho_3}\left(\frac{F}{A_F E_F}\right)^2}}{B_1 + \frac{1}{\sqrt{K_{CE}\rho_3}}\left(\frac{F}{A_F E_F}\right)}\right] + \frac{2\pi.j}{\sqrt{K_{CE}\rho_3}} \qquad (43)$$

The negative root is used again, and j is chosen to five the first solution with $\ell_D > \ell_1$. s_{LD} is found from equation (39).

3.3.3 Primary, degradation and secondary zones present

All zones present when the slip of the loaded end exceeds s_2, the shape and length of the primary and secondary zones remain constant.

The combined length of the elastic and degradation zone (ℓ_2) can be found using (42):

(42) gives

$$\ell_2 = \frac{2}{\sqrt{K_{CE}\rho_3}} \tan^{-1}\left[\frac{B_1 - \sqrt{B_1^{\,2} + B_2^{\,2} - (s_{LD} - \rho_2/\rho_3)^2}}{B_2 + s_{LD} - \rho_2/\rho_3}\right] + \frac{2\pi.j}{\sqrt{K_{CE}\rho_3}} \qquad (44)$$

At the boundary between the degradation and friction zones:

(40) gives $$\left(\frac{ds}{dx}\right)_{L2} = \sqrt{K_{CE}\rho_3}\,[B_1 \cos(\ell_2\sqrt{K_{CE}\rho_3}) - B_2 \sin(\ell_2\sqrt{K_{CE}\rho_3})] \qquad (45)$$

As equation (3) indicates, the bond-stress at the friction zone is constant. The governing of the friction zone is:

$$\frac{d^2 s}{dx^2} = K\tau_2 \qquad (17)\text{bis}$$

Where, $$K = K_{CE} = \frac{4}{\phi E_F}\left[1 + \frac{A_F E_F}{A_C E_C}\right] \quad \text{(for the situation of this thesis)} \qquad (14)\text{bis}$$

(14), (17) give $$\frac{d^2 s}{dx^2} = K_{CE}\tau_2 \qquad (46)$$

The slip can be calculated by integrating the equation (46):

$$s = \frac{K_{CE}\tau_2 x^2}{2} + B_3 x + B_4 \qquad (47)$$

The constants B3 and B4 are calculated by applying the boundary conditions $s = s_2$ and equation (45) at $x = \ell_2$:

$$B_3 = \sqrt{K_{CE}\rho_3}\,[B_1 \cos(\ell_2\sqrt{K_{CE}\rho_3}) - B_2 \sin(\ell_2\sqrt{K_{CE}\rho_3})] - K_{CE}\tau_2\ell_2 \qquad (48)$$

$$B_4 = s_2 - \frac{K_{CE}\tau_2\ell_2^{\,2}}{2} - B_3\ell_2 \qquad (49)$$

The boundary at the loaded end ($x = \ell_D$) gives:

(18) gives $$\ell_D = -\frac{B_3}{K_{CE}\tau_2} + \sqrt{(\frac{B_3}{K_{CE}\tau_2})^2 - \frac{2(B_4 - s_{LD})}{K_{CE}\tau_2}} \quad (50)$$

(22) gives $$F = \frac{A_F E_F A_C E_C}{A_F E_F + A_C E_C}\sqrt{B_3{}^2 - 2K_{CE}\tau_2(B_4 - s_{LD})} \quad (51)$$

4. Conclusions

For the long-embedded length, the governing equation is solved under the condition that the disturbed length (ℓ_D) does not exceed the embedded length (ℓ_E). However, for the short-embedded length test, since the bond is relatively weak, the free end of the rod starts to move in extremely short time after the tensile load is applied to the rod, which means the disturbed length increases to the embedded length in no time; this does not allow the governing equations of the short-embedded length case to be solved using boundary condition directly, because the boundary condition at the free end of the rod (equation (22)) is no longer suitable.

In this paper, the analytical bond stress-slip curve (Modified-B.E.P. model) of the short embedded length specimen is not found by solving the equations using boundary conditions at first, but by well-fitting the three parts of the Modified-B.E.P. model which are governed by equations (1), (2) and (3) with the experimental curves.

References

[1] Stratford T.J., Burgoyne C.J., 2003, Shear Analysis of Concrete with Brittle Reinforcement, ASCE Journal of Composites in Construction, 7/4, 323-330

[2] Vicente Alcaraz Carrillo de Albornoz et al. Experimental Study of a New Strengthening Technique of RC Beams Using Prestressed NSM CFRP Bars. Sustainability, 2019, 11(5): 1374.

[3] Laura De Lorenzs et al, Bond of Fiber-Reinforced Polymer Laminates to Concrete, ACI Material Journal, V. 98, No. 3 2001, pp. 256-264.

[4] Chen. J.F., and Teng. J.G., 2001, Anchorage Strength Model for FRP and Steel Plates Bonded to concrete, Journal of Structural Engineering, ASCE, Vol.127, No.7, July, pp.784-791.

[5] Boulebd Adel et al. Modeling of CFRP strengthened RC beams using the SNSM technique, proposed as an alternative to NSM and EBR techniques. Fracture and Structural Integrity, 2020, 14(54): 21 - 35.

[6] Mohammad Abdallah et al. Experimental study on strengthening of RC beams with Side Near Surface Mounted technique-CFRP bars. Composite Structures, 2020, 234(C): 111716-111716.

[7] W.K.K.G. Kalupahana and T.J. Ibell and A.P. Darby. Bond characteristics of near surface mounted CFRP bars. Construction and Building Materials, 2013, 43: 58-68.

[8] Ahmed H. Abdel-Kareem. Punching Strengthening of Concrete Slab-column Connections Using Near Surface Mounted (NSM) Carbon Fiber Reinforced Polymer (CFRP) Bars. Journal of Engineering Research and Reports, 2020: 1-14.

[9] Tamer Eljufout and Houssam Toutanji. Fatigue behavior of prefatigued reinforced concrete beams rehabilitated with near surface mounted carbon fiber reinforced polymer reinforcement. Structural Concrete, 2020, 21(2):533-547.

[10] AlZu'bi Mohammad et al. The effect of length and inclination of carbon fiber reinforced polymer laminates on shear capacity of near-surface mounted retrofitted reinforced concrete beams. Structural Concrete, 2021, 22(6):3677-3691.